Journal of Experimental Botany Advance Access published August 4, 2015

Journal of Experimental Botany
doi:10.1093/jxb/erv381

RESEARCH PAPER

AtCOX10, a protein involved in haem *o* synthesis during cytochrome *c* oxidase biogenesis, is essential for plant embryogenesis and modulates the progression of senescence

Natanael Mansilla, Lucila Garcia, Daniel H. Gonzalez and Elina Welchen*

Instituto de Agrobiotecnología del Litoral (CONICET-UNL), Cátedra de Biología Celular y Molecular, Facultad de Bioquímica y Ciencias Biológicas, Universidad Nacional del Litoral, Centro Científico Tecnológico Santa Fe - Colectora Ruta Nacional Nº 168 Km 0, Paraje El Pozo, 3000 Santa Fe, Argentina

* To whom correspondence should be addressed. E-mail: ewelchen@fbcb.unl.edu.ar

Received 25 June 2015; Revised 25 June 2015; Accepted 16 July 2015

Editor: John Lunn

Abstract

Cytochrome *c* oxidase (CcO) biogenesis requires several accessory proteins implicated, among other processes, in copper and haem *a* insertion. In yeast, the farnesyltransferase Cox10p that catalyses the conversion of haem *b* to haem *o* is the limiting factor in haem *a* biosynthesis and is essential for haem *a* insertion in CcO. In this work, we characterized AtCOX10, a putative Cox10p homologue from *Arabidopsis thaliana*. AtCOX10 was localized in mitochondria and was able to restore growth of a yeast Δ*cox10* null mutant on non-fermentable carbon sources, suggesting that it also participates in haem *o* synthesis. Plants with T-DNA insertions in the coding region of both copies of *AtCOX10* could not be recovered, and heterozygous mutant plants showed seeds with embryos arrested at early developmental stages that lacked CcO activity. Heterozygous mutant plants exhibited lower levels of CcO activity and cyanide-sensitive respiration but normal levels of total respiration at the expense of an increase in alternative respiration. AtCOX10 seems to be implicated in the onset and progression of senescence, since heterozygous mutant plants showed a faster decrease in chlorophyll content and photosynthetic performance than wild-type plants after natural and dark-induced senescence. Furthermore, complementation of mutants by expressing *AtCOX10* under its own promoter allowed us to obtain plants with T-DNA insertions in both *AtCOX10* copies, which showed phenotypic characteristics comparable to those of wild type. Our results highlight the relevance of haem *o* synthesis in plants and suggest that this process is a limiting factor that influences CcO activity levels, mitochondrial respiration, and plant senescence.

Key words: Cytochrome *c* oxidase, embryo lethality, haem *a* synthesis, mitochondrial biogenesis, respiratory complex, senescence.

Introduction

Energy production through oxidative phosphorylation is one of the main processes that take place inside mitochondria. Oxidative phosphorylation is performed by the sequential operation of complexes (I–V) located in the inner mitochondrial membrane. These complexes use the reductive power stored in organic compounds for the synthesis of

Abbreviations: BN-PAGE, blue-native polyacrylamide gel electrophoresis; CcO, cytochrome c oxidase; CLSM, confocal laser scanning microscopy; DAB, 3,3′-diaminobenzidine; GAPC, cytosolic glyceraldehyde-3-phosphate dehydrogenase; GFP, green fluorescent protein; GUS, β-glucuronidase; mRFP, monomeric red fluorescent protein; mt-GFP, GFP in mitochondria; ROS, reactive oxygen species; RT-qPCR, reverse transcription quantitative real-time PCR; SHAM, salicylhydroxamic acid.

ATP. Complex IV or cytochrome *c* oxidase (CcO) is a multimeric Cu–haem *a* terminal oxidase that catalyses electron transfer from cytochrome *c* to O_2. CcO is composed of three highly conserved hydrophobic subunits encoded by mitochondrial DNA in most species (COX1, COX2, and COX3). The remaining structural components (11–13 in different eukaryotes; Khalimonchuk and Rödel, 2005) are encoded in the nucleus, synthesized in the cytosol, and imported into mitochondria by the TOM/TIM import machinery (Neupert and Herrmann, 2007). CcO activity also depends on the presence of metallic co-factors and prosthetic groups (Cu atoms, haem *a*, and Mg^{2+}, Zn^{2+}, and Na^{+} ions), which are required for the proper assembly of a stable and functional enzyme (Barrientos *et al.*, 2009; Soto *et al.*, 2012). COX1, the biggest subunit, contains one haem *a* and a binuclear centre formed by one haem a_3 and a Cu_B centre, responsible for the reduction of O_2 to water. The binuclear Cu_A centre present in COX2 constitutes the entry site for electrons carried on by cytochrome *c* (Poyton and McEwen, 1996). COX3 has no cofactor and is involved in the assembly and stabilization of the enzymatic core (Su *et al.*, 2014). Furthermore, the catalytic core of CcO is surrounded by small nuclear subunits implicated in the stabilization and dimerization of CcO and in the protection of the catalytic centres against deleterious effects produced by reactive oxygen species (ROS) (Fontanesi *et al.*, 2008). In all eukaryotic organisms, inappropriate assembly of CcO subunits leads to a malfunctioning of respiration and ROS production.

Adding more complexity to CcO biogenesis, studies in yeast have unveiled the presence of more than 30 accessory proteins responsible for CcO assembly and function (Thöny-Meyer, 2003; Barrientos *et al.*, 2009). Proteins similar to yeast CcO assembly factors have been studied in *Arabidopsis*, especially those that act as metallo-chaperones responsible for the delivery and insertion of Cu atoms into COX1 and COX2. Thus, AtCOX17 and AtCOX19 are able to complement the respiratory deficiency of *cox17* and *cox19* yeast null mutants, respectively (Balandin and Castresana, 2002; Attallah *et al.*, 2007*a*). More recently, it was demonstrated that disruption of the *AtHCC1* gene, which encodes a Sco1p homologue (Cobine *et al.*, 2006), causes embryo lethality (Attallah *et al.*, 2011; Steinebrunner *et al.*, 2011) and a decrease in CcO activity (Steinebrunner *et al.*, 2014).

Much less is known about the factors involved in the biosynthesis of haem *a* and its insertion into CcO in plants. Haem *a* is an essential cofactor for respiration in a wide range of organisms. Proteins related to haem *a* biosynthesis have been studied in bacteria (Saiki *et al.*, 1992, 1993; Mogi *et al.*, 1994; Brown *et al.*, 2004), yeast (Barros and Tzagoloff, 2002; Wang *et al.*, 2009), *Trypanosoma cruzi* (Buchensky *et al.*, 2010), and humans (Glerum and Tzagoloff, 1994; Pecina *et al.*, 2004). Haem *a* synthesis from haem *b* requires two catalytic steps. First, haem *o* synthase or COX10 transfers a farnesyl group to the C-2 vinyl group of haem *b* (Glerum and Tzagoloff, 1994). In a second reaction, COX15 oxidizes the methyl substituent on pyrrole ring D to an aldehyde, converting haem *o* to haem *a* (Barros *et al.*, 2001; Brown *et al.*, 2002). Because free haem is toxic to the cell, synthesis and insertion of this cofactor should be perfectly coordinated. There are several lines of evidence suggesting the existence of a fine regulation between haem *a* synthesis and its insertion in COX1. While the interaction between Cox10p and Cox15p could not be demonstrated in yeast (Barros and Tzagoloff, 2002), homologous proteins from *Rhodobacter sphaeroides* co-purify when expressed in *Escherichia coli*, suggesting the existence of a physical interaction between both enzymes (Brown *et al.*, 2004).

Like other mutations in CcO assembly factors, haem *a* deficiency causes a complete absence of CcO activity and respiration in yeast (Glerum *et al.*, 1997). In humans, there are reports that different point mutations in COX10 and COX15 cause CcO deficiency and cause Leigh syndrome and hypertrophic cardiomyopathy (Antonicka *et al.*, 2003). Expression of the *COX10* gene is regulated by the microRNA miR-210, which is induced under hypoxia or Fe deficiency in order to reduce COX10 levels and thus regulates the rate of oxygen consumption and mitochondrial metabolism (Chan *et al.*, 2009).

In this work, we characterized the *Arabidopsis* haem *o* synthase homologue AtCOX10. By complementation analysis, we showed that AtCOX10 was able to restore respiratory activity in a yeast Δ*cox10* null mutant. In plants, AtCOX10 is located in mitochondria and is essential for plant survival, since knockout of its gene caused embryo lethality. Heterozygous mutant plants exhibited lower CcO activity levels and alterations in mitochondrial respiration with an increased proportion of cyanide-resistant O_2 consumption. In addition, AtCOX10 seems to influence the progression of senescence, since heterozygous mutants showed an increased rate of chlorophyll loss and photosynthesis decay during both natural and dark-induced senescence. Our results highlight the relevance of adequate haem *o* synthase activity for CcO function and mitochondrial respiration and its impact on plant developmental processes.

Materials and methods

Plant material and growth conditions

Arabidopsis thaliana Heyhn. ecotype Columbia (Col-0) was purchased from Lehle Seeds (Tucson, AZ, USA). The *AtCOX10* T-DNA insertion mutant line SAIL_1283_D03.V1 was obtained from the *Arabidopsis* Biological Resource Centre, Ohio State University, OH, USA. The location of the T-DNA insertion and the presence of the wild-type allele in *AtCOX10*/*Atcox10* plants were determined using specific primers (see Supplementary Table S2, available at *JXB* online) in PCRs on genomic DNA. For protein localization by confocal laser scanning microscopy (CLSM), *Arabidopsis* line *mt-gk* (NASC ID N16263; Nelson *et al.*, 2007), provided by the Nottingham *Arabidopsis* Stock Centre, was used. Plants were grown on soil in 8 cm diameter, 7 cm height pots at 22–24 °C under long-day conditions (16 h light/8 h darkness) at an intensity of approximately 100 µmol m^{-2} s^{-1}. Alternatively, *Arabidopsis* seeds were surface sterilized in a solution containing 70% (v/v) ethanol and 0.1% (w/v) SDS for 5 min, washed in distilled water, and sown in Petri dishes containing 0.5× Murashige and Skoog medium and 1% (w/v) agar. Plates were cold stratified at 4 °C for 2 d and transferred to a growth chamber under long-day conditions.

Gene cloning and generation of transgenic Arabidopsis *lines*

To obtain plants expressing a fusion of AtCOX10 to monomeric red fluorescent protein (mRFP), a 1328 bp *Bam*HI/*Xho*I fragment comprising the entire *AtCOX10* coding sequence was amplified from a cDNA clone (RAFL19-72-F12) using specific oligonucleotides (Supplementary Table S2) and cloned into pENTR 3C (Life Technologies). This fragment, together with its flanking recombination sites, was amplified by PCR and transferred to the destination binary vector pGWB554 (Nakagawa *et al.*, 2007), using the Gateway cloning system (Life Technologies). This vector allows C-terminal fusions of proteins to mRFP or mCherry under the control of the enhanced cauliflower mosaic virus 35S promoter. The construct was introduced into line *mt-gk* (Nelson *et al.*, 2007) expressing green fluorescent protein (GFP) in mitochondria (mt-GFP). T1 seedlings resistant to kanamycin (from the pGWB554 vector) and hygromycin (from the marker line) were used for confocal microscopy.

To obtain *Arabidopsis* plants expressing *AtCOX10* promoter:*gus* fusions, a fragment spanning nt –533 to +95 relative to the transcription start site of *AtCOX10* was obtained by PCR amplification of *Arabidopsis* genomic DNA using specific oligonucleotides (Supplementary Table S2). The resulting fragment was cloned into the binary vector pBI101.3 in front of the β-glucuronidase (*GUS*) gene coding region. T3 homozygous plants resistant to kanamycin (from the pBI101.3 vector) were used to analyse the expression of the reporter gene by optical microscopy. GUS activity was analysed by histochemical staining using the chromogenic substrate 5-bromo-4-chloro-3-indolyl-β-D-glucuronic acid as described by Hull and Devic (1995).

To obtain plants that express *AtCOX10* under its own promoter, a 1328 bp *Bam*HI/*Sac*I fragment comprising the entire *AtCOX10* coding sequence was amplified from cDNA clone RAFL19-72-F12 using specific oligonucleotides (Supplementary Table S2) and cloned downstream of the At*COX10* promoter in replacement of the *GUS* coding region of the vector described in the previous paragraph.

For plant transformation, *Agrobacterium tumefaciens* strain LBA4404 transformed with the respective constructs was used to obtain transgenic *Arabidopsis* plants by the floral dip procedure (Clough and Bent, 1998). Fifteen positive independent lines for each construct were used to select homozygous T3 and T4 plants in order to analyse phenotypes and expression levels. Transgenic seedlings were selected with 50 mg l^{-1} of kanamycin on plates or 0.1% ammonium glufosinate (BASTA) on soil (for SAIL_1283_D03.V1 plants).

Complementation of a Δcox10 *yeast mutant with* AtCOX10

For complementation of a yeast *cox10* mutant strain, a 1328 bp *Bam*HI/*Hin*dIII fragment comprising the entire At*COX10* coding sequence was amplified from cDNA clone RAFL19-72-F12 using specific oligonucleotides (Supplementary Table S2) and cloned into yeast expression vector pMV611 (Wang, *et al.*, 2004). Constructs with the insert and the empty plasmid were introduced into the yeast *cox10* null mutant strain BY4742/Δ*cox10* (BY4742; Matα; his3Δ1; leu2Δ0; lys2Δ0; ura3Δ0; YHL019c::kanMX4), obtained from EUROSCARF, using the standard lithium acetate transformation method. Clones able to grow on minimal medium without leucine were checked for the presence of the plasmid by PCR and then tested for growth on fermentable (YPD: 2% glucose, 1% yeast extract, 2% peptone) or non-fermentable (YEPG: 3% glycerol, 2% ethanol, 1% yeast extract, 2% peptone) medium. The parent strain BY4742 (Matα; his3Δ1; leu2Δ0; lys3Δ0; ura3Δ0) was used as a positive control of growth.

CLSM

For CLSM, roots of 7-d-old plants were imaged in water with a Zeiss LSM 780 confocal laser scanning microscope as described in detail by Steinebrunner *et al.* (2014). For co-localization analyses, intensity-scatter plots were generated with the 'Coloc 2' and 'Colocalization Threshold' plug-ins of the Fiji software (Schindelin *et al.*, 2012).

RNA isolation and analysis

RNA samples were prepared with Trizol (Invitrogen). Reverse transcription quantitative real-time PCR (RT-qPCR) analysis was performed according to O'Connell (2002). First-strand cDNA synthesis was performed using an oligo$(dT)_{18}$ primer and Moloney murine leukemia virus reverse transcriptase (Promega) under standard conditions. Quantitative PCR was performed on an aliquot of the cDNA synthesis reaction with specific primers (Supplementary Table S2). RT-qPCR was carried out using an MJ Research Chromo4 apparatus. Expression values were normalized using *PP2AA3* or *ACT2* and *ACT8* transcript levels as standards (Charrier *et al.*, 2002; Czechowski *et al.*, 2005).

Respiration measurements

For oxygen consumption, plants were kept in darkness for 40 min and then the fourth, fifth and sixth leaves were transferred to 2.5 ml of reaction buffer [300 mM mannitol, 1% (w/v) BSA, 10 mM potassium phosphate (pH 7.2), 10 mM KCl, 5 mM $MgCl_2$]. Measurements were made at 25 °C using a Clark-type oxygen electrode (Hansatech, Norfolk, UK). The capacity of the CcO pathway was determined as the O_2 uptake sensitive to 1 mM KCN in the presence of 10 mM salicylhydroxamic acid (SHAM). The capacity of the alternative pathway was determined as the O_2 uptake sensitive to 10 mM SHAM in the presence of 1 mM KCN (Welchen *et al.*, 2012). Oxygen consumption in yeast was measured at an OD_{600}=0.6 in YPD medium and in a 2 ml final volume.

Blue-native polyacrylamide gel electrophoresis (BN-PAGE) of mitochondria-enriched extracts

Extracts enriched in mitochondrial proteins were prepared from seedlings grown for 10 d under a 16 h light/8 h darkness photoperiod in liquid Murashige and Skoog medium as described by Steinebrunner *et al.* (2011, 2014). Proteins from crude mitochondrial fractions were separated by BN-PAGE according to the protocol described by Wittig *et al.* (2006). Digitonin (detergent:protein ratio of 4:1) was used for membrane protein solubilization. Equal amounts of mitochondrial proteins, as deduced from citrate synthase activity measurements, were loaded in each lane. Proteins were visualized by Coomassie Brilliant Blue colloidal staining (Neuhoff *et al.*, 1988). CcO activity staining was performed as described by Steinebrunner *et al.* (2014). The brown precipitate indicating CcO activity was followed over time.

Western blot analysis

For Western blot analysis, proteins prepared from crude mitochondrial fractions were separated by SDS-PAGE and transferred to Hybond-ECL (GE Healthcare). Blots were probed with polyclonal rabbit antibodies against AtCOX2 or AtVDAC1 (Agrisera) at a dilution of 1:2500 and developed with anti-rabbit immunoglobulin conjugated with horseradish peroxidase using the SuperSignal® West Pico Chemiluminescent Substrate (Pierce).

Determination of chlorophyll content and visual inspection of senescence

Visual inspection of senescence was based on leaf yellowing. The onset of senescence was determined when the tip of the first leaf acquired a yellow colour,and complete senescence was when the entire plant was yellow. Chlorophyll content was measured spectrophotometrically as described by Porra (2002). Results are expressed as the chlorophyll content (g of fresh weight)$^{-1}$.

For dark-induced senescence, the fourth and fifth leaves of plants (four plants for each genotype and incubation time) were collected and incubated in darkness in 5 mM phosphate buffer (pH 5.7) at 23 °C for 0 to 7 d. After this, samples were collected for visual inspection and chlorophyll measurement.

Measurement of photosynthetic parameters

Fluorescence in leaves was measured using a Li-6400 portable photosynthetic system (Li-Cor). Prior to measurements, each leaf was allowed to adapt for 60 min in darkness and four to five biological measurements were made using different plants for each genotype.

Microscopic inspection of developing embryos

Siliques were fixed in 1% paraformaldehyde and then cleared for 2 h in Hoyer's solution containing 100 g of chloral hydrate, 2.5 g of Arabic gum and 5 ml of glycerol in 30 ml of water. Cleared seeds at different developmental stages were observed using a Nikon E800 microscope with Nomarski optics and photographed with a Nikon DXM1200 camera.

Histochemical analysis of CcO and cytosolic glyceraldehyde-3-phosphate dehydrogenase (GAPC) activity in embryos

Histochemical analysis was made as described Attallah *et al.* (2011). GAPC (EC 1.2.1.12) activity was assayed as described previously (Piattoni *et al.*, 2013) with modifications necessary for *in situ* histochemistry of *Arabidopsis* embryos (Baud and Graham, 2006). Fixed embryos were incubated in reaction buffer containing 50 mM Tricine/NaOH (pH 8.5), 1 mM NAD^+, 10 mM sodium arsenate, 0.4 U aldolase (rabbit muscle), 1.2 mM fructose-1,6-bisphosphate and 0.8 mM nitroblue tetrazolium. For the negative control, fructose-1,6-bisphosphate was omitted from the reaction. Embryos were analysed in a Nikon E200 microscope and photographed using a Panasonic DMC-F3 camera.

Sequence alignment and phylogenetic tree analysis

Protein sequences corresponding to plant homologues of Cox10p from *Saccharomyces cerevisiae* were downloaded from Phytozome 9.1 (http://www.phytozome.net/) (Goodstein *et al.*, 2012). Sequences corresponding to other organisms were searched using the standard protein blast (BlastP: http://blast.ncbi.nlm.nih.gov/Blast.cgi) from the National Center for Biotechnology Information. Sequence alignment was made using default parameters established in the WebPRANK alignment server (Löytynoja and Goldman, 2012). Maximum-likelihood tree reconstruction with the best model and 1000 bootstrap pseudoreplicates was run using the software Seaview 4.5.0 and the algorithm PhyML-aLRT(SH-LIKE) with 100 random starts. The tree was represented using the FigTree v1.4.0 software (Gouy *et al.*, 2010).

Statistical analysis

Data were analysed by one-way analysis of variance and the means were compared by Tukey or Fisher (LSD) tests. Statistical analysis was performed using InfoStat Version 2013 for Windows (http://www.infostat.com.ar).

Results

Identification and characterization of an Arabidopsis COX10 *homologue*

A survey of sequences with similarity to yeast COX10p allowed us to identify putative COX10 homologues in organisms from all life domains including archea and eubacteria, indicating that COX10 is an ancestral protein, key for cellular respiration. This is probably due to the role of COX10 in haem *a* synthesis, necessary for respiration in all organisms that contain aa_3 terminal oxidases. COX10 protein sequences from 39 organisms were used to assemble a phylogenetic tree (Supplementary Fig. S1, available at *JXB* online). This showed a clear separation between COX10 sequences from all kingdoms in different clades. Only one copy of putative *COX10* gene sequences seemed to be present in most genomes. The exception occurred in plants, where the divergence in two gene copies encoding COX10, probably arising from independent duplication events, was noticeable in *Zea mays*, *Glycine max*, *Brassica rapa*, and *Panicum virgatum* (Supplementary Fig. S1). The copies from *Z. mays* and *G. max* were divergent from their paralogues, possibly indicating a recent neofunctionalization process. Otherwise, duplicated genes from *Brassica* and *Panicum* showed high sequence similarity, indicating that they probably arose from a recent duplication process.

The putative COX10 protein from *Arabidopsis* (AtCOX10) had 431 aa, compared to 462 and 443 for the proteins from yeast and humans, respectively. An analysis of COX10 protein sequences from humans, yeast, and *Arabidopsis* indicated that essential residues responsible for function of the enzymes from humans and yeast were conserved in the *Arabidopsis* protein (Fig. 1A, vertical arrows). Yeast and human COX10 are integral inner membrane proteins with eight to nine predicted transmembrane helices (Nobrega *et al.*, 1990). AtCOX10 also shared this characteristic showing nine putative membrane-spanning domains that perfectly match those described for humans and yeast (data not shown). These observations suggested that *Arabidopsis* AtCOX10 may fulfil a function comparable to those described for the human and yeast COX10 proteins.

AtCOX10 is able to complement a yeast cox10 *null mutant.*

In order to analyse whether AtCOX10 is effectively able to replace the function of yeast Cox10p, we performed a complementation assay of a yeast *cox10* null mutant. To do this, we transformed a yeast Δ*cox10* mutant with a construct expressing the *AtCOX10* cDNA under the strong constitutive *GPD* promoter (Mumberg *et al.*, 1995). We observed that *AtCOX10* expression was able to restore growth of the Δ*cox10* null mutant on non-fermentable carbon sources, although at levels not strictly comparable to those of the wild-type strain used as control (Fig. 1B). We also evaluated the respiratory capacity of yeast cells complemented with the plant protein using a Clark-type oxygen electrode. While Δ*cox10* cells transformed with the empty vector showed oxygen consumption rates near zero, confirming that Cox10p is necessary for normal respiratory activity in yeast (Nobrega *et al.*, 1990), cells transformed with the construct expressing the *Arabidopsis* protein showed respiratory values of about 20–25% relative to wild-type cells (Fig. 1C). Our results showed that AtCOX10 is able to restore, although only partially, respiration of a yeast *cox10* null mutant, suggesting that the plant protein has haem *o* synthase activity and is able to participate in CcO assembly in yeast.

AtCOX10 *is localized to the plant mitochondria* in vivo

To accomplish a role in CcO biogenesis, it is expected that AtCOX10 is localized to mitochondria, as for its homologues

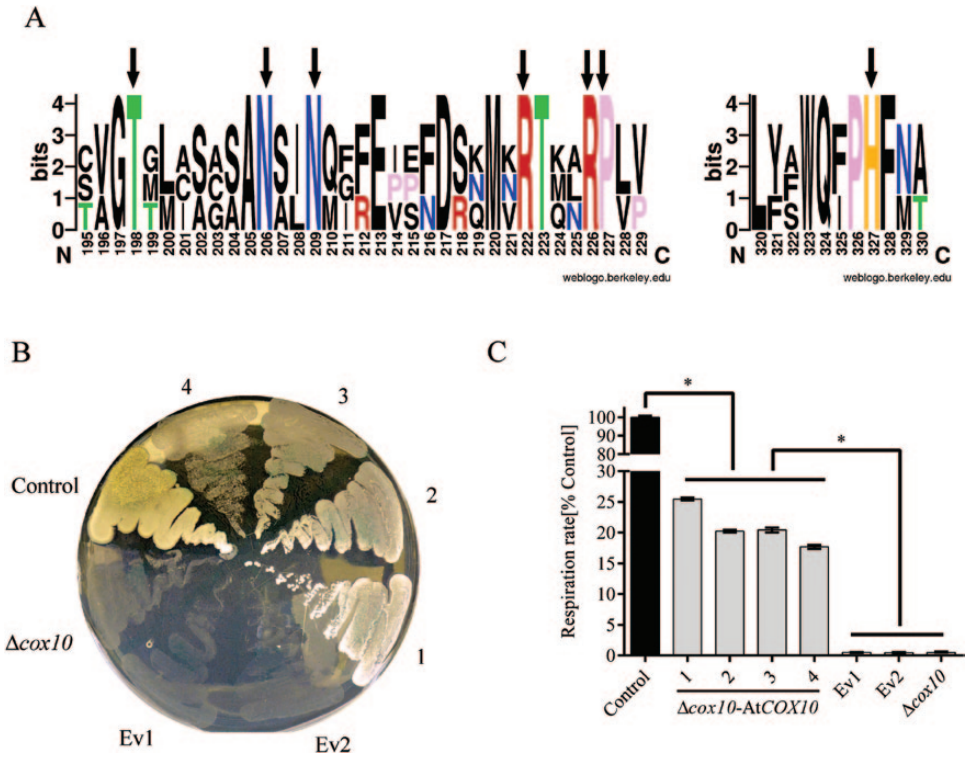

Fig. 1. AtCOX10 functionally complements a yeast Δ*cox10* mutant. (A) WEBLogo based on a sequence alignment made with ClustalW2.0 using *Homo sapiens*, *S. cerevisiae*, and *A. thaliana* COX10 proteins. AtCOX10 shares conserved amino acid residues (indicated by vertical arrows) previously reported as essential for haem *a* synthesis and CcO activity in yeast and humans. (B) Yeast complementation assay: Δ*cox10* yeast cells were transformed with a construct expressing *AtCOX10* under the control of a constitutive promoter. Different clones (1–4) of transformed mutant cells (Δ*cox10-AtCOX10*) were able to grow on non-fermentable carbon sources. As controls, wild-type yeast cells (Control) and Δ*cox10* cells transformed with the empty vector (Ev1, Ev2) were used. (C) Oxygen consumption rates in wild-type cells (Control), several clones of complemented cells (1–4), cells transformed with the empty vector (Ev1, Ev2), and Δ*cox10* mutant cells.

from other eukaryotic organisms. Indeed, mitochondrial localization can be inferred from most subcellular localization prediction programs (Heazlewood *et al.*, 2007). To obtain experimental evidence supporting mitochondrial localization, AtCOX10 was C-terminally tagged with mRFP and expressed in the *Arabidopsis mt-gk* line, expressing GFP in mitochondria (mt-GFP; Nelson *et al.*, 2007). Several lines co-expressing AtCOX10–mRFP and mt-GFP were analysed by CLSM. In all of them, the GFP fluorescence of the mostly dot-shaped mitochondria co-localized with the mRFP fluorescence (Fig. 2), indicating that AtCOX10–mRFP is present in mitochondria. As a control, the intracellular localization of the mRFP tag alone was examined in the *mt-gk* background. In this case, the mRFP signal appeared in the cytosol and no longer co-localized with the GFP signal (not shown). This control demonstrated that AtCOX10 provided the mitochondrial targeting information for mRFP, and that co-localization of the mt-GFP and AtCOX10–mRFP signal was not a crosstalk artefact of the GFP and mRFP detection channels.

AtCOX10 *is expressed in embryos, endosperm, and meristematic regions*

To analyse the expression pattern of *AtCOX10*, we fused the *uidA* (*GUS*) reporter gene to a 628 bp fragment (–533 to +95) corresponding to the putative *AtCOX10* promoter region. Histochemical detection of GUS activity in *Arabidopsis* plants transformed with this construct revealed expression in the first and second leaf pairs (Fig. 3A, B). GUS expression was also observed in vascular root tissues and at the root tip (Fig. 3C). In flowers, expression was evident in the pollen sac and pollen grains, and weakly at the base of sepals (Fig. 3D). Expression was also observed in the endosperm at specific stages of seed development (Fig. 3E-G). The expression pattern conferred by the *AtCOX10* promoter was similar to that described for other genes encoding mitochondrial proteins involved in CcO assembly (Auger *et al.*, 2001) or other mitochondrial activities (Chen *et al.*, 2014).

Inspection of the *AtCOX10* promoter region using the PLACE (http://www.dna.affrc.go.jp/PLACE/), AGRIS (http://arabidopsis.med.ohio-state.edu/) and PlantCare (http://bioinformatics.psb.ugent.be/webtools/plantcare/html/) databases (Higo *et al.*, 1999; Lescot *et al.*, 2002; Palaniswamy *et al.*, 2006) showed the presence of several motifs that may be related to the observed expression pattern (Fig. 3H, Supplementary Table S1, available at *JXB* online). Among them, two site II elements (position between –174 and –117 from the transcriptional start point), relevants for the expression of genes that encode components of the mitochondrial respiratory chain (Welchen and Gonzalez, 2005; Welchen and Gonzalez, 2006), was found. Also, Lat52 and Lat52/56 motifs (positions –413 and–156, respectively), specific for expression in pollen and the pollen sac (Twell *et al.*, 1991; Muschietti *et al.*, 1994; Eyal *et al.*, 1995), a GCN4 element (position –5;

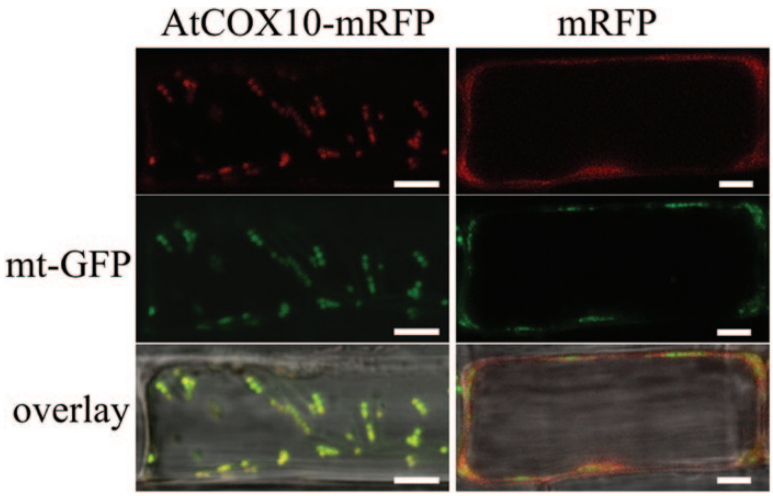

Fig. 2. Subcellular localization of AtCOX10-mRFP. Roots of 7-d-old transgenic lines co-expressing mt-GFP (green) and AtCOX10-mRFP (red) were imaged by CLSM. An exemplary cell is presented in which the signals for the green (A) and red (B) fluorescence channels co-localized as yellow signals when overlaid (C). The overlay includes a bright-field image. Bars, 5 μm.

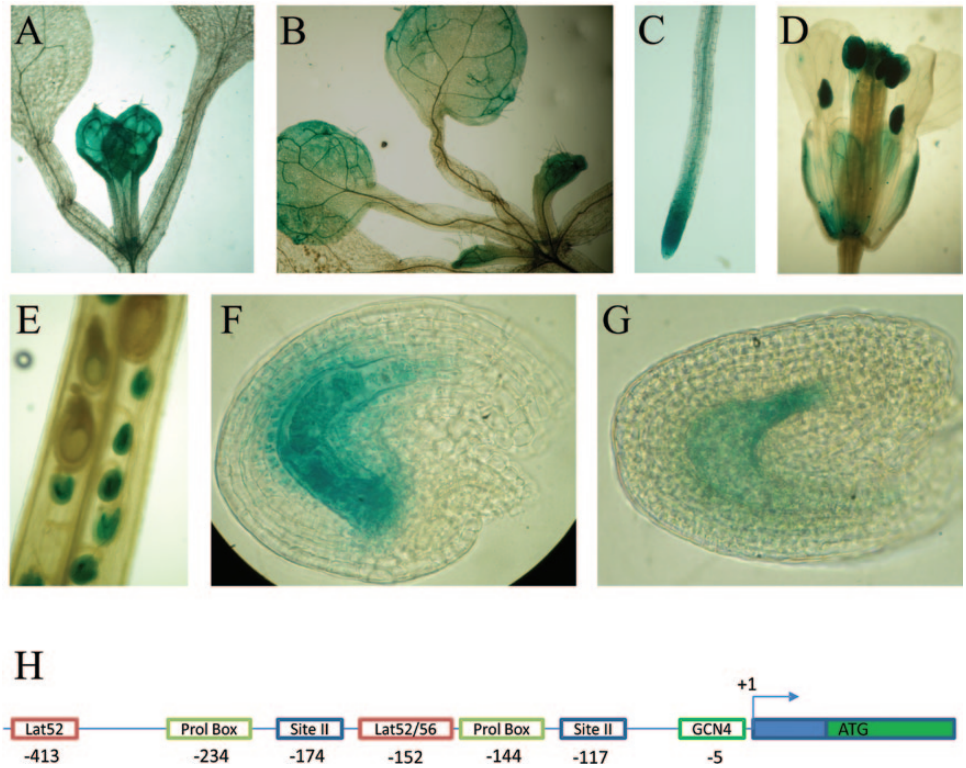

Fig. 3. Analysis of the GUS expression pattern conferred by the *AtCOX10* promoter region. (A–G) Expression was observed in the first and second leaf pairs (A, B), in the root vascular cylinder and tip (C), and in pollen sacs and mature pollen, and weakly at the base of flowers (D). Expression was also detected in seeds (E), more precisely in endosperm at a few days post-fertilization (F, G). GUS expression was not observed in any other tissue or developmental stage. Images were taken with an optical microscope. (H) Schematic representation of the *AtCOX10* promoter region. The different boxes correspond to previously reported elements involved in transcriptional regulation of other genes (see Supplementary Table S1 for details).

Wu *et al.*, 2000) and Prolamin boxes (–234 and –144; Vicente-Carbajosa *et al.*, 1997; Mena *et al.*, 1998), that regulate expression in the endosperm, were observed.

AtCOX10 is essential at early stages of plant development

To elucidate the role of AtCOX10 in plants, we studied an *Arabidopsis* mutant line with a T-DNA insertion in the second exon of the *AtCOX10* gene (Fig. 4A). Homozygous mutant plants for this line could not be identified in successive generations (Supplementary Fig. S2A, available at *JXB* online). Analysis of heterozygous (*AtCOX10/atcox10*) plants revealed that approximately 25% of seeds in their siliques showed abnormal morphology (Supplementary Fig. S2B). Abnormal seeds were smaller and had a brownish colour compared with normal seeds (similar to those of wild-type plants) in the same silique, which looked greener (Fig. 4B).

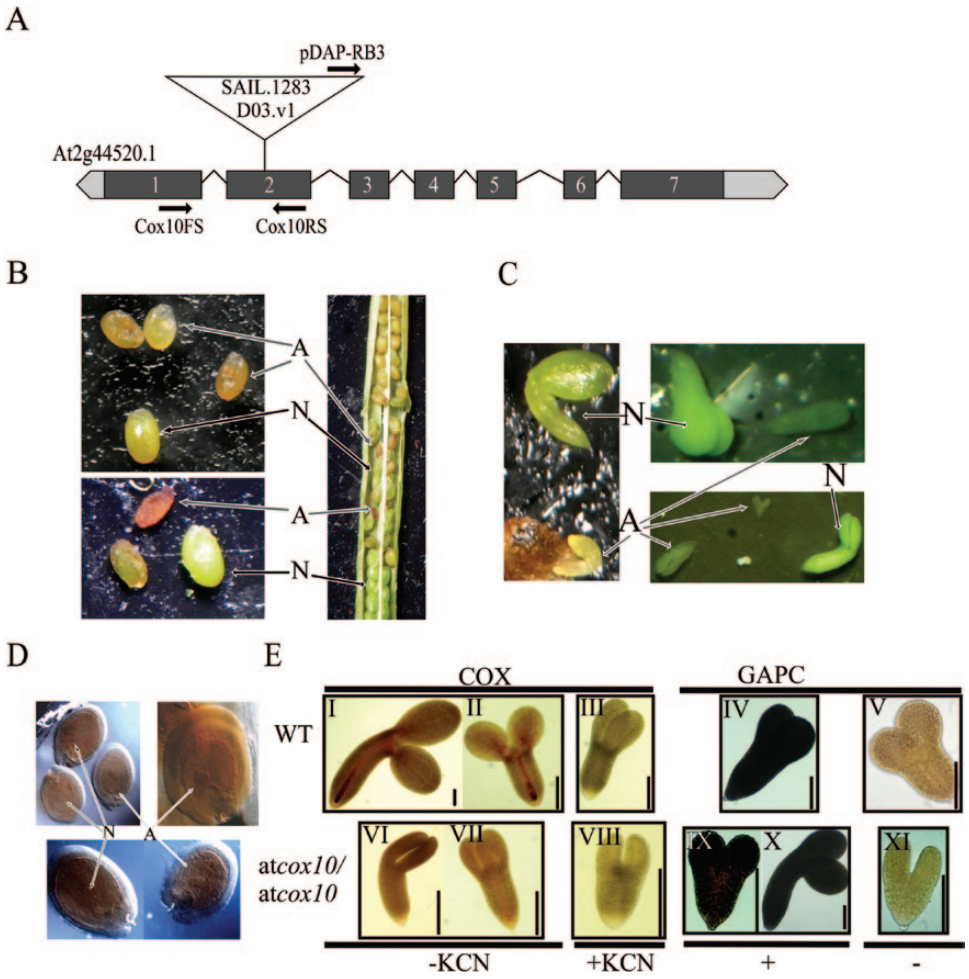

Fig. 4. AtCOX10 is essential for embryogenesis. (A) Schematic representation of the *AtCOX10* gene. The 5′- and 3′-untranslated regions are represented by light grey boxes. Coding regions (exons 1–7) are shaded in dark grey. Thin broken lines represent introns. The position of the T-DNA insertion in the SAIL_1283 mutant line and the oligonucleotides used to determine the presence of mutant or wild-type alleles are shown (see Supplementary Table S2 for primer sequences). (B) Representative silique of an *AtCOX10/atcox10* plant showing normal (N) and abnormal (A) seeds distributed randomly along the silique. (C) Normal (N) and abnormal (A) embryos collected from *AtCOX10/atcox10* plants at different developmental stages. (D) Inspection of embryos using Nomarski microscopy. Note that abnormal embryos (A) are positioned in the centre of the seed, while normal embryos (N) at the torpedo stage are located near the bottom. (E) Histochemical assay of CcO and GAPC activity in embryos from wild-type and *AtCOX10/atcox10* plants. CcO activity was observed as a brown precipitate due to DAB oxidation. GAPC activity was observed as a dark blue precipitate due to nitroblue tetrazolium oxidation. KCN (10 mM) was added to inhibit CcO activity; (–) indicates a negative control of the GAPC reaction in which fructose-1,6-bisphosphate was omitted.

Immature abnormal seeds contained embryos that stopped their development at most at the torpedo stage (Fig. 4C). Using Nomarski microscopy, we observed that the size of the endosperm was decreased in abnormal seeds (Fig. 4D). In addition, embryos in abnormal seeds were positioned near the centre, whereas in normal seeds they were located near the base of seeds (Fig. 4D).

Embryo development is an energy-demanding process. Accordingly, the embryo-lethal phenotype of *atcox10* mutants may be indicative of its essential role in CcO biogenesis. To answer this, we performed histochemical detection of CcO activity using 3,3′-diaminobenzidine (DAB) as substrate in embryos at similar developmental stages from wild-type and normal and abnormal seeds from heterozygote mutant plants before abortion. In the presence of DAB, embryos from normal seeds produced a brown precipitate, indicative of DAB oxidation, in the developing vascular system of roots and cotyledons (Fig. 4E, panels I and II). Embryos from abnormal seeds showed a very weak staining (Fig. 4E, panels VI, and VII), suggesting that homozygous *atcox10* mutant embryos had very low CcO activity compared with wild-type embryos. To confirm that DAB staining was indicative of CcO activity, we used KCN, a known CcO inhibitor, in the reaction buffer. We observed that KCN abolished the appearance of the brown precipitate in embryos (Fig. 4E, panels III and VIII), indicating that DAB oxidation arises from CcO activity. To evaluate whether abnormal embryos contained other enzymatic activities, we performed histochemical detection of GAPC activity. Abnormal embryos showed wild-type levels of GAPC activity (Fig. 4E, panels IV, IX, and X), suggesting that the lack of CcO activity was not due to a general decrease in enzyme levels. According to these observations, we assumed that AtCOX10 is required for CcO biogenesis and that embryo lethality is probably a consequence of decreased

energy availability for cell proliferation and development due to very low levels of CcO activity.

To effectively analyse whether embryo lethality is due to mutation of the *AtCOX10* gene, we performed a complementation assay of the *Arabidopsis Atcox10* mutant. We transformed *Arabidopsis* heterozygous mutant plants with a construct expressing the *AtCOX10* cDNA under its own promoter. After transformation and proliferation of the plants, we were able to isolate plants with T-DNA insertions in both copies of *AtCOX10* (Supplementary Fig. S2D) and showing 100% of seeds with a normal phenotype (Supplementary Fig. S2C). This showed that embryo lethality was due to lack of a functional *AtCOX10* gene in the mutant embryos.

A partial decrease in AtCOX10 *expression affects CcO activity*

To evaluate further the importance of AtCOX10 in CcO biogenesis and mitochondrial respiration, we analysed respiratory parameters and CcO activity in *AtCOX10*/*atcox10* mutant plants. *AtCOX10* transcript levels in these plants were approximately 50% those of wild type (Fig. 5A). In imbibed seeds isolated from heterozygous plants, total respiration rates were similar to those measured in wild-type plants (Fig. 5B). However, these values were reached at the expense of a slight increase in alternative or SHAM-sensitive respiration and a consequent decrease in cyanide-sensitive (CcO-dependent) respiration (Fig. 5B). We measured the same parameters in fully expanded rosette leaves of 4-week-old plants. At this stage, the decrease in cyanide-sensitive respiration in *AtCOX10*/*atcox10* plants, together with the increase in alternative respiration, was more pronounced (Fig. 5C). Again, total respiration was similar to that of wild type.

To directly analyse CcO activity levels, we performed in-gel activity staining of BN-PAGE gels loaded with mitochondria-enriched protein extracts prepared from wild-type and heterozygous mutant plants. After staining, we detected a decrease in CcO activity in *AtCOX10*/*atcox10* mutant plants compared with wild type (Fig. 5D), suggesting that the decrease in cyanide-sensitive respiration observed at the tissue level in *AtCOX10*/*Atcox10* plants was due to lower CcO activity. Complemented *Atcox10*/*Atcox10* mutant plants, on the other hand, showed CcO activity levels comparable to those of wild-type plants (Supplementary Fig. S3, available at *JXB* online). This result confirmed that decreased CcO activity in *AtCOX10*/*Atcox10* plants was due to a deficiency in *AtCOX10*. In parallel, we ran a denaturing gel to evaluate COX2 and VDAC1 protein levels. The levels of these proteins were similar in all samples analysed (Fig. 5E). COX2 levels were similar in wild-type and heterozygous mutant plants, probably due to the presence of unassembled COX2 subunits in mitochondrial extracts, since it has been shown that the levels of mitochondria-encoded subunits do not always correlate with the amount of assembled complexes (Giegé *et al.*, 2005).

A decrease in AtCOX10 *expression affects the onset and progression of natural senescence*

We performed a detailed phenotypic characterization of heterozygous *AtCOX10*/*atcox10*, complemented and wild-type plants. These plants were morphologically indistinguishable along most developmental stages. Parameters such as rosette diameter, flowering time, and flowering stem elongation, among others analysed, were similar to those of wild type (Supplementary Fig. S4, available at *JXB* online). As described in a previous section, one of the parameters that was affected is seed production, since *AtCOX10*/*atcox10* plants, but not wild-type or complemented plants, showed siliques with abnormal seeds. In addition, heterozygous mutants showed early senescence compared with wild-type plants (Fig. 6A). Careful examination of the process indicated that the rosettes of heterozygous plants were completely senescent approximately 7 d before wild-type plants

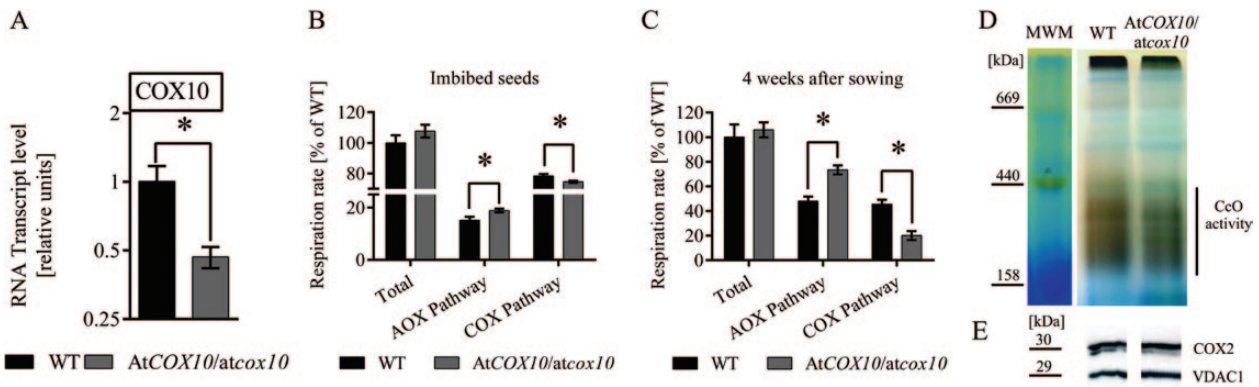

Fig. 5. *AtCOX10*/*Atcox10* plants show decreased CcO activity and cyanide-sensitive respiration. (A) *AtCOX10* transcript levels in 20-d-old rosette leaves from wild-type (WT) (black) and *AtCOX10*/*atcox10* (dark grey) plants. (B, C) Respiration rates (represented as percentage oxygen consumption relative to wild type) were quantified in imbibed seeds (B) and rosette leaves of 4-week-old plants (C) using a Clark-type O_2 electrode. The capacity of the CcO pathway was determined as the O_2 uptake sensitive to 1 mM KCN in the presence of 10 mM SHAM. The alternative pathway capacity was measured as the O_2 uptake after adding 10 mM SHAM in the presence of 1 mM KCN. Asterisks indicate significant differences compared with wild type ($P<0.05$). (D) CcO activity staining of mitochondrial protein extracts from wild-type and *AtCOX10*/*atcox10* plants after separation by BN-PAGE. Mitochondria-enriched protein extracts corresponding to equal amounts of citrate synthase activity, used as a standard of the amount of mitochondria, were loaded in each lane. (E) Western blots with antibodies against COX2 and VDAC1.

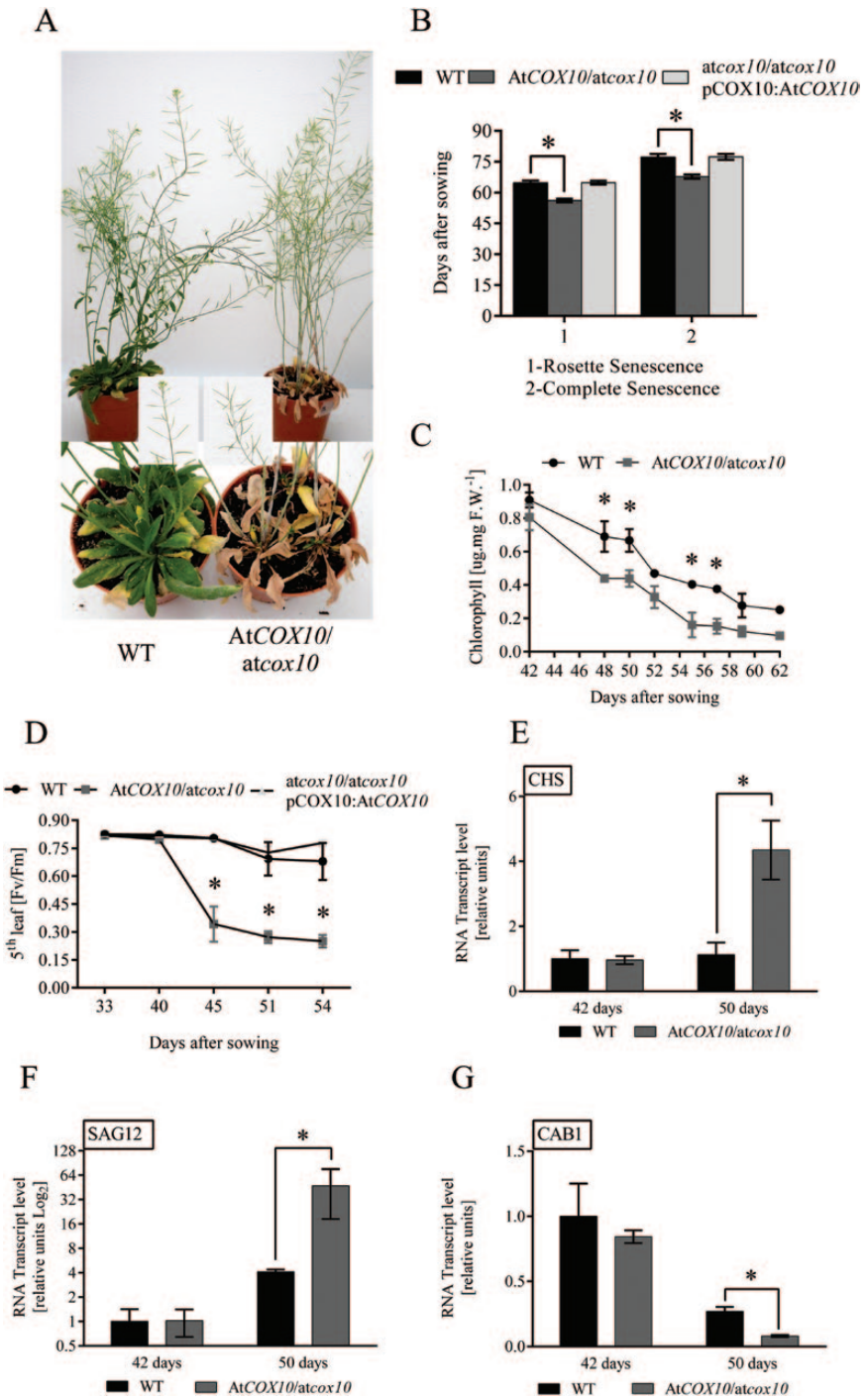

Fig. 6. *AtCOX10/atcox10* plants show accelerated senescence. (A) Phenotype of 50-d-old wild-type and *AtCOX10/atcox10* plants grown under long-day photoperiod. (B) Evolution of senescence in wild-type, *AtCOX10/atcox10*, and complemented (*Atcox10/atcox10* p*COX10:AtCOX10*) plants. The number of days after sowing required for the onset (1) or completion of senescence (2) was determined by visual inspection. (C) Chlorophyll content measured at different days after sowing. (D) Changes in Fv/Fm measured in the fifth leaf at different days after sowing. (E–G) Transcript levels of senescence markers *CHS*, *SAG12* (induced during senescence) and *CAB1* (repressed during senescence) were measured by RT-qPCR in total RNA from wild-type (WT) and *AtCOX10/Atcox10* plants at days 42 and 50 after sowing. Asterisks indicate significant differences ($P<0.05$).

reached a similar stage (Fig. 6B). Progression of senescence in complemented *Atcox10*/*Atcox10* plants was similar to wild type (Fig. 6B), indicating that accelerated senescence was due to At*COX10* deficiency.

To further characterize senescence progression, we measured the chlorophyll content of entire rosettes at days 42–62 after sowing. While at day 42 the chlorophyll content of wild-type and *AtCOX10*/*Atcox10* plants was not significantly different, at day 55 heterozygous plants reached almost full senescence and minimum chlorophyll levels, while wild-type plants still had about 50% of initial chlorophyll levels (Fig. 6C). Since senescence progresses differently in leaves of different ages, we measured the chlorophyll fluorescence parameter Fv/Fm in individual leaves as an indicator of the

performance of photosystem II. The results for the fifth rosette leaf indicate that *AtCOX10*/*atcox10* plants already showed a pronounced decrease in Fv/Fm to values around 0.30 at day 45 after sowing, while no decrease was observed in wild-type and complemented plants up to day 54 (Fig. 6D). The Fv/Fm values obtained for all rosette leaves at days 33, 40, 45, and 54 after sowing are shown in Supplementary Fig. S5A (available at *JXB* online). Leaves 1 and 2 from *AtCOX10*/*atcox10* plants already showed signs of senescence at day 33, when complemented and wild-type leaves had photosynthetic characteristics of healthy plants. Measurements at days 40–54 also clearly showed that the onset of senescence in different leaves occurred earlier in *AtCOX10*/*atcox10* plants (Supplementary Fig. S5A). Another parameter strictly related to AtCOX10 function that may be affected during senescence is respiration. To evaluate this, we measured total, cyanide-sensitive, and alternative respiration in leaves at weeks 5 and 6 after sowing. As observed in plants before senescence (Fig. 5C), no significant differences were observed in total respiration, but *AtCOX10*/*atcox10* plants showed a relative increase in alternative respiration and a similar decrease in cyanide-sensitive respiration (Supplementary Fig. S5B).

We also analysed the response of *AtCOX10*/*atcox10* mutants to dark-induced senescence. To do this, we incubated detached rosette leaves at the same developmental stage in darkness over several days, following the protocol described by Guo and Crawford (2005). As an indication of senescence, we analysed leaves phenotypically and measured their chlorophyll content. According to both parameters, heterozygous plants were more sensitive than wild type to dark-induced senescence (Supplementary Fig. S6, available at *JXB* online).

In order to evaluate senescence at the molecular level, we measured the expression of previously characterized senescence marker genes by RT-qPCR. Transcript levels of *CHALCONE SYNTHASE* (*CHS*) and *SENESCENCE-ASSOCIATED GENE 12* (*SAG12*), two genes induced under senescence conditions (Guo *et al.*, 2004; Buchanan-Wollaston *et al.*, 2005), were similar to wild type at day 42 but increased considerably in heterozygous plants at day 50 after sowing (Fig. 6E, F). In turn, transcript levels of *LIGHT-HARVESTING CHLOROPHYLL-PROTEIN COMPLEX II SUBUNIT B1* (*LHCB1.4*, *CAB1*), which encodes a component of photosystem II that is repressed during senescence (van der Graaff *et al.*, 2006), decreased faster in *AtCOX10*/*atcox10* plants (Fig. 6G). Accelerated senescence in *AtCOX10*/*atcox10* plants thus is also reflected by these changes in gene expression.

Discussion

CcO biogenesis is a strictly controlled sequential process that involves several ancillary proteins called CcO assembly factors (Nijtmans *et al.*, 1998; Fontanesi *et al.*, 2008). While the process is finely described in yeast and there is a wealth of information in humans due to the importance of this process for human health (Valnot *et al.*, 2000; Antonicka *et al.*, 2003), little information is available about CcO biogenesis in plants, perhaps because lethality resulting from CcO deficiency precludes detailed studies. In addition, since plants have an alternative respiratory pathway that drives electrons to O_2 without the participation of CcO, the negative effects of minor CcO deficiencies may be mitigated and remain unnoticed. Until now, knowledge about the regulation of the expression of structural subunits encoded in the nucleus (Welchen *et al.*, 2004; Comelli *et al.*, 2009, 2012) and on factors involved in copper transport and incorporation into CcO (Attallah *et al.*, 2007*a*, *b*, 2011; Steinebrunner *et al.*, 2014) has been available, but nothing is known about haem *a* synthesis and insertion into CcO in plants. Because free haem is toxic to cells and haem *a* is involved in essential steps during electron transport from cytochrome *c* to molecular oxygen, haem *a* synthesis and delivery should be strictly controlled and coordinated. In all organisms where haem *a* synthesis was studied, this pathway is performed by the sequential participation of COX10 and COX15 proteins (haem *o* and haem *a* synthase, respectively) with the help of other proteins characterized mainly in yeast and humans, responsible for the final insertion of the cofactor into COX1. Mutations in human *COX10* lead to CcO-deficient patients with Leigh syndrome, leukodystrophy, and infantile encephalocardiomyopathy (Valnot *et al.*, 2000; Bestwick *et al.*, 2010), showing the importance of COX10 for CcO assembly.

While in eukaryotes COX10 is located in mitochondria, the protein is also present in prokaryotes that contain *aa3*-type CcOs, indicating that this protein is probably universally involved in haem *a* synthesis. In the case of *Arabidopsis*, the results presented here suggest that AtCOX10 is a mitochondrial protein in plants as well.

AtCOX10 is able to replace its homologue in yeast

Complementation of yeast cells deficient in Cox10p with AtCOX10 restores the ability of mutants to growth on non-fermentable carbon sources. Cells complemented with AtCOX10 reach 20–25% the respiratory rate of wild-type cells, while O_2 consumption is negligible in the mutant. This suggests that AtCOX10 can replace its yeast homologue, although only partially. Sequence comparisons between COX10 proteins from humans, yeast, and *Arabidopsis* indicate that, whereas amino acids critical for catalytic activity (Valnot *et al.*, 2000; Bestwick *et al.*, 2010; Buchensky *et al.*, 2010) are conserved, the sequence identity of the proteins is only about 34%. Sequence identity is particularly low in the N-terminal portion of the proteins, which contains the presequence necessary for import into mitochondria. According to this, one possibility is that AtCOX10 is not efficiently imported and processed in yeast. Another important aspect is that Cox10p is active as a complex in the inner membrane of yeast mitochondria (Bestwick *et al.*, 2010; Khalimonchuk *et al.*, 2010). CcO assembly factor Coa2p is responsible for Cox1p haemylation, but for this to happen Cox10p needs to form high-molecular-mass complexes through the interaction with the C-terminal domain of Cox1p (Pierrel *et al.*, 2008; Khalimonchuk *et al.*, 2010, 2012). Coa2p is crucial in coupling the presence of newly synthesized Cox1p to Cox10p

oligomerization (Khalimonchuk *et al.*, 2010, 2012). We were not able to find putative *Arabidopsis* homologues for Coa2p or for Coa1p, Coa3p, Mss51p, and Cox14p, all accessory proteins necessary for Cox1p insertion into the inner mitochondrial membrane of yeast (Bestwick *et al.*, 2010; Fontanesi *et al.*, 2010; Khalimonchuk *et al.*, 2010, 2012). Considering that COX10 establishes a wealth of protein–protein interactions in the inner mitochondrial membrane and is also involved in haem *a* insertion, in addition to its synthesis, the most likely explanation for the lack of full restoration of respiratory capacity is that AtCOX10 may not be able to optimally interact with its partners in yeast. In addition, the simultaneous expression of AtCOX10 and AtCOX15 in Δ*cox10* cells did not increase the respiratory rate beyond the rate observed with AtCOX10 alone (data not shown), suggesting that Cox15p is not the limiting factor. Altogether, our results suggest that AtCOX10 is able to participate in the synthesis of haem *a* and may also be important for the assembly and insertion of this cofactor into COX1.

AtCOX10 is expressed in tissues of high energy demand

The expression pattern conferred by the promoter region of *AtCOX10* is similar to those described for several nuclear genes encoding mitochondrial respiratory proteins (Elorza *et al.*, 2004; Welchen *et al.*, 2004; Welchen and Gonzalez, 2005; Comelli *et al.*, 2009; Attallah *et al.*, 2011). Moreover, analysis of *cis* regulatory elements located in the *AtCOX10* promoter region indicated the presence of site II elements (TGGGCC/T), frequently present in nuclear genes encoding respiratory chain components (Welchen and Gonzalez, 2005, 2006; Gonzalez *et al.*, 2007; Giraud *et al.*, 2010). The *AtCOX10* promoter also drives expression in the endosperm. Furthermore, *AtCOX10* is expressed during phase II of embryo development, between the globular and heart stages (http://www2.bri.nrc.ca/plantembryo/). This phase is characterized by extensive morphogenesis and meristematic tissue development, and energy provided by mitochondria may be relevant for the process. Elements like GCN4 and the Prolamin box, responsible for expression of genes during endosperm development (Vicente-Carbajosa *et al.*, 1997; Wu *et al.*, 2000), are also present in the *AtCOX10* promoter. Expression in meristematic regions and leaf primordia may be related to high energy demands due to high rates of cellular proliferation, as described for nuclear genes encoding mitochondrial proteins. The expression pattern conferred by the *AtCOX10* promoter region agrees with the putative function of AtCOX10 in haem *a* synthesis and insertion in CcO, in order to ensure suitable energy production by mitochondrial respiration.

Lack of AtCOX10 is embryo lethal

We performed a functional analysis of AtCOX10 through the study of an insertional mutant. We observed that homozygous mutants with no functional *AtCOX10* were not viable. While lack of AtCOX10 caused embryo arrest at the heart or torpedo stage, complementation of the mutant by the expression of *AtCOX10* under the control of its own promoter was enough to restore normal embryo development and seed production. This indicates that AtCOX10 is an essential protein, probably due to its role in haem *a* synthesis and CcO biogenesis. Embryo arrest may be due to insufficient energy production needed for cellular proliferation that takes place during the heart and torpedo stages (Mansfield and Briarty, 1990; Boisnard-Lorig *et al.*, 2001; Guitton *et al.*, 2004). This is supported by the fact that CcO activity was barely detectable in a proportion of embryos from heterozygous mutant plants. Furthermore, during phase III of embryo development, which includes the torpedo and bent stages, metabolic activities are activated. This transition is characterized by high expression of genes encoding proteins involved in glycolysis, the pentose-phosphate pathway, and pyruvate and fatty acid metabolisms (Xiang *et al.*, 2011). All of these cellular activities are energy demanding and are connected to mitochondrial activity. An interruption in the respiratory chain at the level of CcO due to the lack of haem *a* synthesis and/or insertion may entail embryo arrest even in the presence of alternative respiration, since the alternative pathway is not involved in energy production (Finnegan *et al.*, 2004). Supporting this idea, there are several reports of *Arabidopsis* mutant plants defective in the assembly and function of mitochondrial *c*-type cytochromes (Meyer *et al.*, 2005; Welchen *et al.*, 2012), in ancillary proteins for copper insertion into CcO (Attallah *et al.*, 2011; Steinnebrunner *et al.*, 2011), and in PPR proteins required for the expression of mitochondria-encoded CcO subunits (Dahan *et al.*, 2014) showing embryo lethality. Conversely, there are several examples of plants lacking components of complex I that are viable and have minor phenotypic disorders (Meyer *et al.*, 2009, 2011; Haïli *et al.*, 2013; Braun *et al.*, 2014; Zhu *et al.*, 2014), indicating that complex I is dispensable for plant survival.

In addition, defects in respiratory activity may impact on endosperm development. As mentioned, abnormal seeds most likely corresponding to homozygous *Atcox10*/*Atcox10* plants are smaller than wild type and show a rough and smaller endosperm, indicating also the presence of abnormalities in this tissue. The endosperm is formed immediately after fertilization for embryo nutrition and protection (Berger, 2003). As with the embryo, the endosperm also undergoes several cellular and nuclear divisions during maturation; both processes are highly energy demanding and intense metabolic activity takes place during this stage (Xiang *et al.*, 2011).

AtCOX10 deficiency impacts on the onset and progression of senescence

We observed that *AtCOX10* deficiency impacted on the onset and progression of senescence in *Arabidopsis*. Senescence started earlier and progressed faster in *AtCOX10*/*atcox10* plants than in wild-type plants, and this is not observed when mutant plants were complemented with a construct that expressed At*COX10* from its own promoter. Senescence is crucial for plant fitness, in order to ensure successful plant perpetuation. Senescence is considered as an altruistic

process whereby leaves modify their metabolism and remobilize carbon and nitrogen, transferring them to developing seeds (Hopkins *et al.*, 2007). During senescence, the most significant change is chloroplast breakdown, since more than 70% of leaf protein and a high proportion of cellular lipids are present in this organelle (Hoertensteiner and Feller, 2002). In agreement with this, we observed that chlorophyll levels and the maximum efficiency of photosystem II (Fv/Fm), used as markers of senescence, decayed earlier and faster in *AtCOX10*/*atcox10* plants but not in complemented plants. This indicates that chloroplast breakdown is accelerated as a consequence of a deficiency in haem *a* synthesis.

Otherwise, mitochondria and the nucleus are the last compartments to be disassembled during senescence, allowing efficient coordination and energy supply (Nam, 1997; Guo *et al.*, 2004; Keech *et al.*, 2007). During this process, acetyl-CoA is formed in glyoxysomes by β-oxidation of fatty acids generated during membrane degradation (Gut and Matile, 1988; DeBellis *et al.*, 1990; Froman *et al.*, 2000; Page *et al.*, 2001). Acetyl-CoA can be converted to oxaloacetate inside mitochondria in order to enter gluconeogenesis and be used for sucrose synthesis, which is then exported to sink tissues (Eastmond and Graham, 2001; Cornah and Smith, 2002). Since this is an energy-demanding process, it can be speculated that a deficiency in AtCOX10, which causes a decrease in CcO capacity, may cause defects in energy production during senescence. In fact, cyanide-sensitive mitochondrial respiration was affected in *AtCOX10*/*atcox10* plants and this was compensated for by an increase in alternative respiration. This imbalance in respiration may imply that less ATP is produced per unit of carbon oxidized and that increased nutrient consumption is necessary to support the energy demands related to nutrient mobilization. Therefore, accelerated use of reserves may explain why *AtCOX10*/*atcox10* plants senesce faster than wild type. If this is the case, other mutants defective in CcO activity must also show early senescence. Known mutants with a partial decrease in CcO activity include knockdown mutants in genes encoding cytochrome *c* (Welchen *et al.*, 2012) and heterozygous mutants in the CcO assembly factor HCC1 (Steinebrunner *et al.*, 2014). None of these mutants show early senescence, pointing to a more specific role of AtCOX10 in this process. One possibility is that AtCOX10, and not the other proteins, becomes limiting for CcO biogenesis at the onset of senescence. A second possibility is that early senescence is not directly related to decreased CcO capacity but to defects in CcO assembly that lead to the production of assembly intermediates with deleterious effects. Finally, the role of AtCOX10 in senescence progression may be independent of its role in CcO biogenesis. Further studies with available mutants defective in CcO capacity are required to evaluate these possibilities. The facts that in plants there are no other known proteins, besides CcO, that require haem *o* or haem *a* for function and that *AtCOX10*/*atcox10* mutants show a decreased proportion of cyanide-sensitive respiration at the onset of senescence suggest that the role of AtCOX10 in senescence progression is most likely to be related to its role in CcO assembly.

In conclusion, our results indicate that AtCOX10 is a limiting factor for CcO biogenesis in plants and highlight the role of haem *o* synthesis in the modulation of CcO activity levels, mitochondrial respiration, and plant senescence.

Supplementary data

Supplementary data are available at *JXB* online.

Supplementary Fig. S1. Phylogenetic tree of COX10 proteins from different organisms.

Supplementary Fig. S2. Characterization of an At*COX10* T-DNA insertion mutant.

Supplementary Fig. S3. Complementation of the *atcox10* mutation restores CcO activity levels in plants.

Supplementary Fig. S4. Phenotypic parameters in wild-type, At*COX10*/*atcox10*, and complemented plants under normal growth conditions.

Supplementary Fig. S5. Characterization of senescence progression in At*COX10*/*atcox10* plants.

Supplementary Fig. S6. Dark-induced senescence in wild-type and At*COX10*/*atcox10* plants.

Supplementary Table S1. Known *cis* regulatory motifs present in the At*COX10* promoter region.

Supplementary Table S2. List of oligonucleotides used in this study.

Acknowledgements

We are very grateful to Ivan Radin and Iris Steinebrunner (TU Dresden, Germany) for generating the transgenic mRFP-expressing *Arabidopsis* lines and for help with the confocal microscopy studies, respectively. The subcellular localization studies were carried out in the Light Microscopy Facility of the Biotechnology Centre, TU Dresden, which provided the confocal laser scanning microscope and excellent training and technical assistance. We also thank Dr Vanesa Piattoni for assistance with the GAPC histochemical assay. Vectors pGWB554 and pMV611 were kindly provided by Drs Tsuyoshi Nakagawa (Shimane University, Matsue, Japan) and Michael Volkert (University of Massachusetts, MA, USA). This project was supported by grants from CONICET (Consejo Nacional de Investigaciones Científicas y Técnicas, Argentina), ANPCyT (Agencia Nacional de Promoción Científica y Tecnológica, Argentina), and Universidad Nacional del Litoral. A stay of EW in Dresden was supported by a collaborative CONICET-DFG (Deutsche Forschungsgemeinschaft) collaborative grant. DHG and EW are members of CONICET. NM and LG are fellows of the same institution.

References

Antonicka H, Leary SC, Guercin GH, Agar JN, Horvath R, Kennaway NG, Harding CO, Jaksch M, Shoubridge EA. 2003. Mutations in COX10 result in a defect in mitochondrial heme A biosynthesis and account for multiple early onset clinical phenotypes associated with isolated COX deficiency. *Human Molecular Genetics* **12,** 2693–2702.

Attallah CV, Welchen E, Gonzalez DH. 2007*a*. The promoters of *Arabidopsis thaliana* genes AtCOX17-1 and -2, encoding a copper chaperone involved in cytochrome *c* oxidase biogenesis, are preferentially active in roots and anthers and induced by biotic and abiotic stress. *Physiologia Plantarum* **129,** 123–134.

Attallah CV, Welchen E, Martin AP, Spinelli SV, Bonnard G, Palatnik JF, Gonzalez DH. 2011. Plants contain two SCO proteins that are differentially involved in cytochrome c oxidase function and copper and redox homeostasis. *Journal of Experimental Botany* **62,** 4281–4294.

Attallah CV, Welchen E, Pujol C, Bonnard G, Gonzalez DH. 2007b. Characterization of *Arabidopsis thaliana* genes encoding functional homologues of the yeast metal chaperone Cox19p, involved in cytochrome *c* oxidase biogenesis. *Plant Molecular Biology*. **65,** 343–355.

Auger DL, Newton KJ, Birchler JA. 2001. Nuclear gene dosage effects upon the expression of maize mitochondrial genes. *Genetics* **157,** 1711–1721.

Balandin T, Castresana C. 2002. AtCOX17, an *Arabidopsis* homolog of the yeast copper chaperone COX17. *Plant Physiology* **129,** 1852–1857.

Barrientos A, Gouget K, Horn D, Soto IC, Fontanesi F. 2009. Suppression mechanisms of COX assembly defects in yeast and human: insights into the COX assembly process. *Biochimica et Biophysica Acta*. **1793,** 97–107.

Barros MH, Carlson CG, Glerum DM, Tzagoloff A. 2001. Involvement of mitochondrial ferredoxin and Cox15p in hydroxylation of heme O. *FEBS Letters* **492,** 133–138.

Barros MH, Tzagoloff A. 2002. Regulation of the heme A biosynthetic pathway in *Saccharomyces cerevisiae*. *FEBS Letters* **516,** 119–123.

Baud S, Graham IA. 2006. A spatiotemporal analysis of enzymatic activities associated with carbon metabolism in wild-type and mutant embryos of *Arabidopsis* using in situ histochemistry. *The Plant Journal* **46,** 155–169.

Berger F. (2003). Endosperm: the crossroad of seed development. *Current Opinion in Plant Biology*. **6,** 42–50.

Bestwick M, Khalimonchuk O, Pierrel F, Winge DR. 2010. The role of Coa2 in hemylation of yeast Cox1 revealed by its genetic interaction with Cox10. *Molecular and Cellular Biology*. **30,** 172–185.

Boisnard-Lorig C, Colon-Carmona A, Bauch M, Hodge S, Doerner P, Bancharel E, Dumas C, Haseloff J, Berger F. (2001). Dynamic analyses of the expression of the HISTONE::YFP fusion protein in *Arabidopsis* show that syncytial endosperm is divided in mitotic domains. *The Plant Cell*. **13,** 495–509.

Braun HP, Binder S, Brennicke A, *et al.* 2014. The life of plant mitochondrial complex I. *Mitochondrion* **19,** 295–313.

Brown KR, Allan BM, Do P, Hegg EL. 2002. Identification of novel hemes generated by heme *a* synthase: evidence for two successive monooxygenase reactions. *Biochemistry* **41,** 10906–10913.

Brown KR, Brown BM, Hoagland E, Mayne CL, Hegg EL. 2004. Heme A synthase does not incorporate molecular oxygen into the formyl group of heme A. *Biochemistry* **43,** 8616–8624.

Buchanan-Wollaston V, Page T, Harrison E, *et al.* 2005. Comparative transcriptome analysis reveals significant differences in gene expression and signaling pathways between developmental and dark/starvation-induced senescence in *Arabidopsis*. *The Plant Journal*. **42,** 567–85.

Buchensky C, Almiron P, Mantilla BS, Silber AM, Cricco JA. 2010. The *Trypanosoma cruzi* proteins TcCox10 and TcCox15 catalyze the formation of heme A in the yeast *Saccharomyces cerevisiae*. *FEMS Microbiology Letters* **312,** 133–141.

Chan SY, Zhang Y, Hemann C, Mahoney CE, Zweier JL, Loscalzo J. 2009. MicroRNA-210 controls mitochondrial metabolism during hypoxia by repressing the iron-sulfur cluster assembly proteins ISCU1/2. *Cell Metabolism* **10,** 273–284.

Charrier B, Champion A, Henry Y, Kreis M. 2002. Expression profiling of the whole *Arabidopsis* shaggy-like kinase multigene family by real-time reverse transcriptase-polymerase chain reaction. *Plant Physiology* **130,** 577–590.

Chen J, Zeng B, Zhang M, Xie S, Wang G, Hauck A, Lai J. 2014. Dynamic transcriptome landscape of maize embryo and endosperm development. *Plant Physiology* **166,** 252–264.

Clough SJ, Bent AF. (1998). Floral dip: a simplified method for *Agrobacterium*-mediated transformation of *Arabidopsis thaliana*. *The Plant Journal* **16,** 735–743.

Cobine PA, Pierrel F, Winge DR. 2006. Copper trafficking to the mitochondrion and assembly of copper metalloenzymes. *Biochimica et Biophysica Acta* **1763,** 759–772.

Comelli RN, Viola IL, Gonzalez DH. 2009. Characterization of promoter elements required for expression and induction by sucrose of the *Arabidopsis* COX5b-1 nuclear gene, encoding the zinc-binding subunit of cytochrome *c* oxidase. *Plant Molecular Biology* **69,** 729–743.

Comelli RN, Welchen E, Kim HJ, Hong JC, Gonzalez DH. 2012. Delta subclass HD-Zip proteins and a B-3 AP2/ERF transcription factor interact with promoter elements required for expression of the *Arabidopsis* cytochrome *c* oxidase 5b-1 gene. *Plant Molecular Biology* **69,** 729–743.

Cornah JE, Smith SM. 2002. Synthesis and function of glyoxylate cycled enzymes. In: Baker A, Graham IA, eds. *Plant peroxisomes*. London, UK: Kluwer Academic Publishers, 57–101.

Czechowski T, Stitt M, Altmann T, Udvardi MK, Scheible WR. 2005. Genome-wide identification and testing of superior reference genes for transcript normalization in *Arabidopsis*. *Plant Physiology* **139,** 5–17.

Dahan J, Tcherkez G, Macherel D, Benamar A, Belcram K, Quadrado M, Arnal N, Mireau H. 2014. Disruption of the *CYTOCHROME C OXIDASE DEFICIENT1* gene leads to cytochrome c oxidase depletion and reorchestrated respiratory metabolism in *Arabidopsis*. *Plant Physiology* **166,** 1788–1802.

DeBellis L, Picciarelli P, Pistelli L, Alpi A. 1990. Localization of glyoxylate-cycle marker enzymes in peroxisomes of senescent leaves and green cotyledons. *Planta* **180,** 435–439.

Eastmond PJ, Graham IA. 2001. Re-examining the role of the glyoxylate cycle in oilseeds. *Trends in Plant Science* **6,** 72–78.

Elorza A, León G, Gómez I, Mouras A, Holuigue L, Araya A, Jordana X. 2004. Nuclear SDH2-1 and SDH2-2 genes, encoding the iron-sulfur subunit of mitochondrial complex II in *Arabidopsis*, have distinct cell-specific expression patterns and promoter activities. *Plant Physiology* **136,** 4072–4087.

Eyal Y, Curi C, McCormick S. 1995. Pollen specificity elements reside in 30 bp of the proximal promoters of two pollen-expressed genes. *The Plant Cell* **7,** 373–384.

Finnegan PM, Soole KL, Umbach AL. 2004. Alternative mitochondrial electron transport proteins in higher plants. In DA Day, AH Millar, J Whelan, eds. *Plant mitochondria: from gene to function*, Vol. **17**. Advances in photosynthesis and respiration. Kluwer, Dordrecht, The Netherlands,163–230.

Fontanesi F, Soto IC, Barrientos A. 2008. Cytochrome c oxidase biogenesis: new levels of regulation IUBMB Life **60,** 557–568.

Fontanesi F, Soto IC, Horn D, Barrientos A. 2010. Mss51 and Ssc1 facilitate translational regulation of cytochrome c oxidase biogenesis. *Molecular and Cellular Biology* **30,** 245–259.

Froman BE, Edwards PC, Bursch AG, Dehesh K. 2000. ACX3, a novel medium-chain acyl-coenzyme A oxidase from *Arabidopsis*. *Plant Physiology* **123,** 733–742.

Giegé P, Lee J, Sweetlove B, Cognat V, Leaver CJ. 2005. Coordination of nuclear and mitochondrial genome expression during mitochondrial biogenesis in *Arabidopsis*. *The Plant Cell* **17,** 1497–1512.

Giraud E, Ng S, Carrie C, Duncan O, Low J, Lee CP, Van Aken O, Millar AH, Murcha M, Whelan J. 2010. TCP transcription factors link the regulation of genes encoding mitochondrial proteins with the circadian clock in *Arabidopsis thaliana*. *The Plant Cell* **22,** 3921–3934.

Glerum DM, Tzagoloff A. 1994. Isolation of a human cDNA for heme A: farnesyltransferase by functional complementation of a yeast *cox10* mutant. *Proceedings of the National Academy of Sciences, USA* **91,** 8452–8456.

Glerum DM, Muroff I, Jin C, Tzagoloff A. 1997. COX15 codes for a mitochondrial protein essential for the assembly of yeast cytochrome oxidase. *Journal of Biological Chemistry* **272,** 19088–19094.

Gonzalez DH, Welchen E, Attallah CV, Comelli RN, Mufarrege EF. 2007. Transcriptional coordination of the biogenesis of the oxidative phosphorylation machinery in plants. *The Plant Journal* **51,** 105–116.

Goodstein DM, Shu S, Howson R, *et al.* 2012. Phytozome: a comparative platform for green plant genomics. *Nucleic Acids Research*. **40,** D1178–D1186.

Gouy M, Guindon S, Gascuel O. 2010. SeaView version 4, A multiplatform graphical user interface for sequence alignment and phylogenetic tree building. *Molecular Biology and Evolution* **272,** 221–224.

Guitton, AE, Page, DR, Chambrier, P, Lionnet C, Faure JE, Grossniklaus U, Berger F. 2004. Identification of new members of fertilization independent seed Polycomb group pathway involved in the control of seed development in Arabidopsis thaliana. *Development* **131,** 2971–2981.

Guo FQ, Crawford NM. 2005. *Arabidopsis* nitric oxide synthase 1 is targeted to mitochondria and protects against oxi-dative damage and dark-induced senescence. *The Plant Cell* **17,** 3436–3450.

Guo Y, Cai Z, Gan S. 2004. Transcriptome of *Arabidopsis* leaf senescence. *Plant, Cell and Environment*. **27,** 521–549.

Gut H, Matile P. 1988. Apparent induction of key enzymes of the glyoxylic acid cycle in senescent barley leaves. *Planta* **176,** 548–550.

Haïli N, Arnal N, Quadrado M, Amiar S, Tcherkez G, Dahan J, Briozzo P, Colas des Francs-Small C, Vrielynck N, Mireau H. 2013. The pentatricopeptide repeat MTSF1 protein stabilizes the *nad4* mRNA in *Arabidopsis* mitochondria. *Nucleic Acids Research* **41,** 6650–6663.

Heazlewood JL, Verboom RE, Tonti-Filippini J, Small I, Millar AH. 2007. SUBA: the *Arabidopsis* Subcellular Database. *Nucleic Acids Research*. **35,** 213–218.

Higo K, Ugawa Y, Iwamoto M, Korenaga T. 1999. Plant *cis*-acting regulatory DNA elements (PLACE) database. *Nucleic Acids Research* **27,** 297–300.

Hoertensteiner S, Feller U. 2002. Nitrogen metabolism and remobilization during senescence. *Journal of Experimental Botany* **53,** 927–937.

Hopkins M, Taylor C, Liu Z, Ma F, McNamara L, Wang TW, Thompson JE. 2007. Regulation and execution of molecular disassembly and catabolism during senescence. *New Phytology* **175,** 201–21.

Hull GA, Devic M. 1995. The β-glucuronidase (GUS) reporter gene system. Gene fusions; spectrophotometric, fluorometric, and histochemical detection. *Methods in Molecular Biology*. **49,** 125–141.

Keech O, Pesquet E, Ahad A, Askne A, Nordvall DAG, Vodnala SM, Tuominen H, Hurry V, Dizengremel P, Gardeström P. 2007. The different fates of mitochondria and chloroplasts during dark-induced senescence in *Arabidopsis* leaves. *Plant, Cell and Environment* **30,** 1523–1534.

Khalimonchuk O, Bestwick M, Meunier B, Watts TC, Winge DR. 2010. Formation of the redox cofactor centers during Cox1 maturation in yeast cytochrome oxidase. *Molecular and Cellular Biology* **30,** 1004–1017.

Khalimonchuk O, Kim H, Watts T, Perez-Martinez X, Winge DR. 2012. Oligomerization of heme o synthase in cytochrome oxidase biogenesis is mediated by cytochrome oxidase assembly factor Coa2. *Journal of Biological Chemistry* **287,** 26715–26726.

Khalimonchuk O, Rödel G. 2005. Biogenesis of cytochrome c oxidase. *Mitochondrion* **5,** 363–388.

Lescot M, Dehais P, Thijs G, Marchal K, Moreau Y, Van de Peer Y, Rouzé P, Rombauts S. 2002. PlantCARE, a database of plant *cis*-acting regulatory elements and a portal to tools for in silico analysis of promoter sequences. *Nucleic Acids Research* **301,** 325–327.

Löytynoja A, Goldman N. 2012. webPRANK: a phylogeny-aware multiple sequence aligner with interactive alignment browser. *Nucleic Acids Research* **11,** 579.

Mansfield SG, Briarty LG. (1990). Development of the free nuclear endosperm in *Arabidopsis thaliana* (L.). *Arabidopsis Information Service*. **27,** 53–64.

Mena M, Vicente-Carbajosa J, Schmidt RJ, Carbonero P. 1998. An endosperm-specific DOF protein from barley, highly conserved in wheat, binds to and activates transcription from the prolamin-box of a native B-hordein promoter in barley endosperm. *The Plant Journal* **16,** 53–62.

Meyer EH, Giegé P, Gelhaye E, Rayapuram N, Ahuja U, Thöny-Meyer L, Grienenberger JM, Bonnard G. 2005. AtCCMH, an essential component of the *c*-type cytochrome maturation pathway in *Arabidopsis* mitochondria, interacts with apocytochrome *c*. *Proceedings of the National Academy of Sciences, USA* **102,** 16113–16118.

Meyer EH, Solheim C, Tanz SK, Bonnard G, Millar AH. 2011. Insights into the composition and assembly of the membrane arm of plant complex I through analysis of subcomplexes in *Arabidopsis* mutant lines. *Journal of Biological Chemistry* **286,** 26081–26092.

Meyer EH, Tomaz T, Carroll AJ, Estavillo G, Delannoy E, Tanz SK, Small ID, Pogson BJ, Millar AH. 2009. Remodeled respiration in ndufs4 with low phosphorylation efficiency suppresses *Arabidopsis* germination and growth and alters control of metabolism at night. *Plant Physiology* **151,** 603–619.

Mogi T, Saiki K, Anraku Y. 1994. Biosynthesis and functional role of haem O and haem A. *Molecular Microbiology* **14,** 391–398.

Mumberg D, Müller R, Funk M. 1995. Yeast vectors for the controlled expression of heterologous proteins in different genetic backgrounds. *Gene* **156,** 119–122.

Muschietti J, Dircks L, Vancanneyt G, McCormick S. 1994. LAT52 protein is essential for tomato pollen development: Pollen expressing antisense LAT52 RNA hydrates and germinates abnormally and cannot achieve fertilization. *The Plant Journal* **6,** 321–338.

Nakagawa T, Suzuki T, Murata S, *et al*. 2007. Improved Gateway binary vectors: high-performance vectors for creation of fusion constructs in transgenic analysis of plants. *Bioscience, Biotechnology, and Biochemistry* **71,** 2095–2100.

Nam, HG. 1997. The molecular genetic analysis of leaf senescence. *Current Opinion in Biotechnology* **8,** 200–207.

Nelson BK, Cai X, Nebenführ A. 2007. A multicolored set of in vivo organelle markers for co-localization studies in *Arabidopsis* and other plants. *The Plant Journal* **51,** 1126–1136.

Neuhoff V, Arold N, Taube D, Ehrhardt W. 1988. Improved staining of proteins in polyacrylamide gels including isoelectric focusing gels with clear background at nanogram sensitivity using Coomassie Brilliant Blue G-250 and R-250. *Electrophoresis* **6,** 255–262.

Neupert W, Herrmann JM. 2007. Translocation of proteins into mitochondria. *Annual Review of Biochemistry* **76,** 723–749.

Nijtmans LGJ, Taanman J W, Muijsers AO, Speijer D, Van den Bogert C. (1998). Assembly of cytochrome-c oxidase in cultured human cells. *European Journal of Biochemistry* **254,** 389–394.

Nobrega MP, Nobrega FG, Tzagoloff A. 1990. COX10 codes for a protein homologous to the ORF1 product of *Paracoccus denitrificans* and is required for the synthesis of yeast cytochrome oxidase. *Journal of Biological Chemistry* **265,** 14220–14226.

O'Connell, J. **(ed.)** 2002. *RT-PCR protocols. Methods in Molecular Biology*, Vol. **193**. Totowa, NJ: Human Press.

Page T, Griffiths G, Buchanan-Wollaston V. 2001. Molecular and biochemical characterization of postharvest senescence in broccoli. *Plant Physiology* **125,** 718–727.

Palaniswamy SK, James S, Sun H, Lamb RS, Davuluri RV, Grotewold E. 2006. AGRIS and AtRegNet: A platform to link cis-regulatory elements and transcription factors into regulatory networks. *Plant Physiology* **140,** 818–829.

Pecina P, Houstková H, Hansíková H, Zeman J, Houstek J. 2004. Genetic defects of cytochrome c oxidase assembly. *Physiological Research* **53,** 213–223.

Piattoni CV, Guerrero SA, Iglesias AA. 2013. A differential redox regulation of the pathways metabolizing glyceraldehyde-3-phosphate tunes the production of reducing power in the cytosol of the plant cells. *International Journal of Molecular Sciences* **14,** 8073–8092.

Pierrel F, Khalimonchuk O, Cobine PA, Bestwick M, Winge DR. 2008. Coa2 is an assembly factor for yeast cytochromecoxidase biogenesis that facilitates the maturation of Cox1. *Molecular and Cellular Biology* **28,** 4927–4939.

Porra RJ. 2002. The chequered history of the development and use of simultaneous equations for the accurate determination of chlorophylls *a* and *b*. *Photosynthesis Research* **73,** 149–156.

Poyton RO, McEwen JE. 1996. Crosstalk between nuclear and mitochondrial genomes. *Annual Review of Biochemistry* **65,** 563–607.

Saiki K, Mogi T, Anraku Y. 1992. Heme O biosynthesis in *Escherichia coli*: the *cyoE* gene in the cytochrome BO operon encodes a protoheme IX farnesyltransferase. *Biochemical and Biophysical Research Communications* **189,** 1491–1497.

Saiki K, Mogi T, Ogura K, Ankaru, Y. 1993. In vitro heme o synthesis by the *cyoE* gene product from *Escherichia coli*. *Journal of Biological Chemistry* **268,** 26041–26045.

Schindelin J, Arganda-Carreras I, Frise E, *et al*. 2012. Fiji: an open-source platform for biological-image analysis. *Nature Methods* **9,** 676–682.

Soto IC, Fontanesi F, Liu J, Barrientos A. 2012. Biogenesis and assembly of eukaryotic cytochrome c oxidase catalytic core. *Biochimica et Biophysica Acta* **1817,** 883–897.

Steinebrunner I, Gey U, Andres M, Garcia L, Gonzalez DH. 2014. Divergent functions of the *Arabidopsis* mitochondrial SCO proteins: HCC1 is essential for COX activity while HCC2 is involved in the UV-B stress response. *Frontiers in Plant Science* **5,** 87.

Steinebrunner I, Landschreiber M, Krause-Buchholz U, Teichmann J, Rödel G. 2011. HCC1, the *Arabidopsis* homologue of the yeast mitochondrial copper chaperone SCO1, is essential for embryonic development. *Journal of Experimental Botany* **62,** 319–330.

Su CH, McStay GP, Tzagoloff A. 2014. The Cox3p assembly module of yeast cytochrome oxidase. *Molecular Biology of the Cell* **25,** 965–976.

Thöny-Meyer L. 2003. A heme chaperone for cytochrome c biosynthesis. *Biochemistry* **42,** 13099–13105.

Twell O, Yamaguchi J, Wing RA, Ushiba J, McCormick, S. 1991. Promoter analysis of genes that are coordinately expressed during pollen development reveals pollen-specific enhancer sequences and shared regulatory elements. *Genes & Development* **5,** 496–507.

Valnot I, von Kleist-Retzow JC, Barrientos A, Gorbatyuk M, Taanman JW, Mehaye B, Rustin P, Tzagoloff A, Munnich A, Rötig A. 2000. A mutation in the human heme A:farnesyltransferase gene COX10 causes cytochrome c oxidase deficiency. *Human Molecular Genetics* **9,** 1245–1249.

van der Graaff E, Schwacke R, Schneider A, Desimone M, Flügge UI, Kunze R. 2006. Transcription analysis of *Arabidopsis* membrane transporters and hormone pathways during developmental and induced leaf senescence. *Plant Physiology* **141,** 776–92.

Vicente-Carbajosa J, Moose SP, Parsons RL, Schmidt RJ. 1997. A maize zinc-finger protein binds the prolamin box in zein gene promoters and interacts with the basic leucine zipper transcriptional activator Opaque2. *Proceedings of the National Academy of Sciences, USA* **94,** 7685–7690.

Wang JY, Sarker AH, Cooper PK, Volkert MR. 2004. The single strand dna binding activity of human PC4 prevents mutagenesis and killing by oxidative DNA damage. *Molecular and Cellular Biology* **24,** 6084–6093.

Wang Z, Wang Y, Hegg EL. 2009. Regulation of the heme A biosynthetic pathway differential regulation of heme A synthase and heme O synthase in *Saccharomyces cerevisiae*. *Journal of Biological Chemistry* **284,** 839–847.

Welchen E, Chan RL, Gonzalez DH. 2004. The promoter of the *Arabidopsis* nuclear gene COX5b-1, encoding subunit 5b of the mitochondrial cytochrome c oxidase, directs tissue-specific expression by a combination of positive and negative regulatory elements. *Journal of Experimental Botany* **55,** 1997–2004.

Welchen E, Gonzalez DH. 2005. Differential expression of the *Arabidopsis* cytochrome c genes *Cytc-1* and *Cytc-2*. Evidence for the involvement of TCP domain protein-binding elements in anther- and meristem-specific expression of the *Cytc-1* gene. *Plant Physiology* **139,** 88–100.

Welchen E, Gonzalez, DH. 2006. Overrepresentation of elements recognized by TCP-domain transcription factors in the upstream regions of nuclear genes encoding components of the mitochondrial oxidative phosphorylation machinery. *Plant Physiology* **141,** 540–545.

Welchen E, Hildebrandt TM, Lewejohann D, Gonzalez DH, Braun HP. 2012. Lack of cytochrome c in *Arabidopsis* decreases stability of Complex IV and modifies redox metabolism without affecting Complexes I and III. *Biochimica et Biophysica Acta* **1817,** 990–1001.

Wittig I, Braun HP, Schägger H. 2006. Blue-native PAGE. *Nature Protocols* **1,** 418–428.

Wu C, Washida H, Onodera Y, Harada K, Takaiwa F. 2000. Quantitative nature of the Prolamin-box, ACGT and AACA motifs in a rice glutelin gene promoter: minimal *cis*-element requirements for endosperm-specific gene expression. *The Plant Journal* **23,** 415–421.

Xiang D, Venglat P, Tibiche C, *et al*. 2011. Genome wide analysis reveals gene expression and metabolic network dynamics during embryo development in *Arabidopsis*. *Plant Physiology* **156,** 346–56.

Zhu Q, Dugardeyn J, Zhang C, *et al*. 2014. The *Arabidopsis thaliana* RNA editing factor SLO2, which affects the mitochondrial electron transport chain, participates in multiple stress and hormone responses. *Molecular Plant* **7,** 290–310.